

MOLECULAR DOCKING AND DYNAMICS OF BIOACTIVE COMPOUNDS DERIVED FROM *Sauropus androgynus* AS CYCLOOXYGENASE-2 INHIBITORS

Aisyah, Wiji Utami, Ayu Faadila*

Chemistry Department, Faculty of Science and Technology, UIN Sulthan Thaha Saifuddin, Jambi, Indonesia

*Corresponding author: wijiutami@uinjambi.ac.id

Abstract

Inflammation is a biological response to injury that can become chronic and lead to various immunological disorders in humans. Bioactive compounds in *Sauropus androgynus* exhibit a broad spectrum of biological activity, including anti-inflammatory effects. This study employed a computational approach involving Lipinski's Rule of Five, protein network analysis, molecular docking, ADMET prediction, molecular dynamics simulations, and Density Functional Theory (DFT) calculations for electronic structure elucidation. Among the tested compounds, corchoionoside C and afzelin demonstrated the strongest inhibitory potential against the COX-2 enzyme, with binding energies of -9.57 and -9.14 kcal/mol, respectively. Molecular dynamics simulations showed that the *S. androgynus* bioactive compound-COX-2 complexes exhibited minimal fluctuation and remained highly stable throughout the simulation, supporting their potential biological activity. DFT HOMO-LUMO analysis further indicated the capability of corchoionoside C and afzelin to interact with biological targets such as COX-2 through polar or electrostatic interactions. These findings are expected to provide a scientific foundation for the development of novel anti-inflammatory agents with promising pharmacological profiles and reduced adverse effects.

Keywords: Bioactive compounds, *Sauropus androgynus*, anti-inflammatory, molecular docking, molecular dynamics.

Introduction

Inflammation plays a significant role in the pathogenesis of various immunological disorders in humans, including neurodegenerative and cardiovascular diseases (Ju et al., 2022). It represents an immune response aimed at eliminating harmful stimuli, regenerating damaged tissue, and restoring biological homeostasis (Jantarawong et al., 2025). Upon stimulation, macrophages produce several inflammatory mediators such as

prostaglandin E2 (PGE2) and nitric oxide (NO). The activation of these immune cells triggers the release of arachidonic acid from cell membranes through the enzyme phospholipase A2 (PLA2), which subsequently becomes the main substrate in the biosynthesis of PGE2 via the cyclooxygenase-2 (COX-2) pathway. COX-2 induction is regulated by various pro-inflammatory cytokines, including interleukin-1 β (IL-1 β), tumor necrosis factor- α (TNF- α), and interleukin-6 (IL-6), acting through nuclear factor-kappa B (NF-

κ B) activation (Lee et al., 2020). PGE2 is one of the primary eicosanoids involved in mediating inflammatory responses and plays a crucial role in vascular permeability, hyperalgesia, and pyrexia. If inflammation is not promptly managed, it may progress from an acute to a chronic condition (Utami et al., 2020). COX-2 inhibitors serve as central targets in non-steroidal anti-inflammatory drug (NSAID) therapy due to their involvement in the pathophysiology of inflammatory diseases.

NSAIDs are among the most widely prescribed medications, accounting for approximately 5–10% of global prescriptions, with more than 30 million individuals estimated to use them daily (McEvoy et al., 2021). Although commonly used to treat inflammation and cancer therapy, prolonged NSAID use can lead to various adverse effects, including gastric ulcers and gastrointestinal bleeding (Chandwe & Kelly, 2021). Around 10% of patients receiving NSAID therapy experience gastrointestinal symptoms such as dyspepsia and gastroesophageal reflux, including heartburn and regurgitation (Tai & McAlindon, 2021). Therefore, the broad spectrum of biological activities present in bioactive constituents from natural sources offers promising alternatives for the development of safer and more effective therapeutic agents.

Sauropus androgynus contains various essential nutrients, including vitamin C, protein, polyphenols, minerals, carotenoids, ascorbic acid, and antioxidants (Awaludin et al., 2020). It is also rich in secondary metabolites such as flavonoids, tannins, alkaloids, steroids, and terpenoids. These bioactive components exhibit antioxidant, antibacterial, and anti-inflammatory potential (Xia et al., 2024). Additionally, the high chlorophyll content in *S. androgynus* contributes to mitigating oxidative stress. Previous studies reported that chlorophyll extracted from *S. androgynus* exerts antioxidant effects in rats induced with NaNO_2 , evaluated through blood and liver parameters. Ananda et al. (2024) found that afzelin from the ethanol extract of *S. androgynus* leaves, evaluated in

silico, has potential as a herbal candidate for COVID-19 treatment. In vitro findings by Hikmawanti et al. (2021) also demonstrated that *S. androgynus* leaves possess antioxidant activity with an IC_{50} value of 88.33 ppm. Thus, *S. androgynus* shows strong pharmacological potential for therapeutic interventions across various diseases.

This study investigates the efficacy of *S. androgynus* bioactive compounds as anti-inflammatory agents using Lipinski's Rule of Five, protein network analysis, molecular docking, ADMET (Absorption, Distribution, Metabolism, Excretion, and Toxicity) screening, and molecular dynamics simulations. The molecular docking analysis focused on the COX-2 receptor (PDB ID: 5IKQ) due to the limited number of studies evaluating the anti-inflammatory potential of *S. androgynus* through in silico approaches. COX-2 is an enzyme that regulates pain during inflammation, and pain remains one of the most distressing symptoms for patients (Yucel et al., 2024). Moreover, COX-2 catalyzes the synthesis of pro-inflammatory prostaglandins, acts as a central stimulator of cancer metastasis progression, and is one of the four key inflammatory mediators alongside PGE2, NF- κ B, and inducible nitric oxide synthase (iNOS) (Trabalzini, 2020; ur Rashid et al., 2019). Molecular dynamics simulations were conducted to validate the docking results and to assess the stability and conformational behavior of the complexes under conditions resembling the human physiological environment (Sinha & Wang, 2022). The findings of this study are expected to provide a scientific foundation for the development of anti-inflammatory agents with improved pharmacological profiles.

Experimental Section

Materials

This in silico study utilized an ACER Laptop-5C7HDF19 equipped with an 11th Gen Intel® Core™ i5-1135G7 @ 2.40–2.42 GHz processor, 8.00 GB RAM (7.78 GB usable), a 64-bit system, and a high-

performance custom-built PC with an AMD AM5 RYZEN 7-7700X 9KY7375W30231 CPU, an AM5 GigaByte B850M Aorus Elite WIFI6E ICE motherboard, and DDR5 SN250950035162 memory. The software used included AutoDockTools 1.5.6 (Morris & Lim-Wilby, 2008), Chimera 1.14 (Pettersen et al., 2004), BIOVIA Discovery Studio Visualizer (Dassault Systemes, 2019), and YASARA Dynamics developed by Bioscience GmbH (Land, Henrik, 2017). The 3D structures of 12 bioactive compounds in *S. androgynus* were downloaded from PubChem (<https://pubchem.ncbi.nlm.nih.gov/>). The compounds were 2,4-Di-tert-butylphenol, afzelin, astragaln, kaempferol, corchoionoside C, trifolin, quercetin, 1-methyl-2-pyrrolidineethanol, favipiravir, 2-acetylpyrrolidine, 2-methoxy-4-vinylphenol, and morpholine (Ananda et al. 2024; Fikri & Purnama, 2020; Gayathiri et al. 2024; Zhang et al. 2017). Meclofenamic acid, the native ligand in this study, was obtained from the RCSB PDB database using PDB ID: 5IKQ (Orlando & Malkowski, 2016). This receptor has a high-resolution X-ray diffraction structure of 2.41 Å. Based on the Ramachandran plot, the structure demonstrated good stereochemical quality, further supported by favorable Verify-3D and ProSA scores (Bommu et al., 2017).

Lipinski's Rule of Five

The Lipinski analysis was performed using the web-based platform at <http://www.scfbio-iitd.res.in/software/drugdesign/lipinski.jsp#anchortag> to predict physicochemical parameters related to drug-likeness. Candidate bioactive compounds must comply with Lipinski's criteria for oral administration in humans. These parameters include molecular weight < 500 Da, log P < 5, ≤10 hydrogen bond acceptors (HBA), and ≤5 hydrogen bond donors (HBD) (Lipinski, 2004).

Protein Network Analysis

Protein network analysis was conducted using the Search Tool for Interactions of Chemicals (STITCH) via its

free web server (<http://stitch.embl.de/>) to identify interactions between *S. androgynus* compounds and human proteins (Kuhn et al., 2008).

Molecular Docking Calculation

The 3D crystal structure of the COX-2 enzyme was obtained from the RCSB PDB database using PDB ID: 5IKQ (Orlando & Malkowski, 2016). Ligand structures were prepared using Chimera 1.14 (Pettersen et al., 2004). Redocking was performed to validate the docking protocol. The grid box size was set to 66 × 66 × 66 with a spacing of 0.375 Å, centered at X = 22.518, Y = 51.524, and Z = 17.635. All bioactive compounds from *S. androgynus* were geometrically optimized using Avogadro with the MMFF94 force field to obtain minimum-energy conformations prior to docking. Docking simulations were conducted using AutoDockTools 1.5.6, running 10 iterations with the Lamarckian Genetic Algorithm. Ligands were treated as flexible, allowing exploration of torsional angles to identify the most favorable binding poses. Ligand-protein interactions were visualized using BIOVIA Discovery Studio 2021 (Dassault Systemes, 2019).

Absorption, Distribution, Metabolism, Excretion, and Toxicity (ADMET)

Pharmacokinetic properties were predicted using ADMET Lab 2.0 (<https://admetmesh.scbdd.com/service/evaluation/index>), covering absorption, distribution, metabolism, excretion, and toxicity parameters. These characteristics are essential in drug discovery, as poor ADMET profiles frequently lead to preclinical or clinical failure. Early prediction improves the success rate of candidate compounds while ensuring safety and efficacy.

Frontier Molecular Orbital (FMO)

Density Functional Theory (DFT) was used to calculate the electronic properties of *S. androgynus* compounds as potential anti-inflammatory drug candidates. The calculations were carried out at the B3LYP/6-31G level of theory

using the ORCA software package and visualized with IboView (Knizia, 2013; Neese et al., 2020).

Molecular Dynamics Simulations

The two compounds with the lowest binding energies from the molecular docking results were selected for molecular dynamics simulations. The simulations were performed using the YASARA Dynamics program developed by Biosciences GmbH (Land, Henrik, 2017). Simulation parameters were set at 310 K and physiological pH 7.4. The simulation time was configured using the md_run macro

with a duration of 100,000 ps (100 ns). The AMBER14 force field was applied (Case, D. A., 2016), with 4000 simulation steps and snapshot saving every 25 ps. The simulation was executed using the md_runfast macro. Root Mean Square Deviation (Cα RMSD), ligand RMSD, total hydrogen bonds, and radius of gyration were analyzed using md_analyze. Meanwhile, Root Mean Square Fluctuation (RMSF) and Molecular Mechanics Poisson–Boltzmann Surface Area (MMPBSA) energies were obtained using md_analyzeres and md_bindenergy, respectively.

Table 1. Results of Lipinski’s Rule of Five for compounds from *Sauropus androgynus*.

No.	Compounds	Lipinski’s Rule of Five					
		Molecular Mass (≤500 Da)	Hydrogen Bond Acceptor (HBA ≤10)	Hydrogen Bond Donor (HBD ≤5)	MlogP	Violation	Drug-likeness
1.	Meclofenamic acid (native ligand)	295.020	3	2	5.133	0	Unviolated
2.	2,4-Di-tert-butylphenol	206.170	1	1	4.832	0	Unviolated
3.	Afzelin	432.110	10	6	1.892	1	Unviolated
4.	Astragalin	448.100	11	7	0.570	2	Violated
5.	Kaempferol	286.050	6	4	2.656		Unviolated
6.	Corchoionoside C	386.190	8	5	0.245	0	Unviolated
7.	Trifolin	448.100	11	7	0.828	2	Violated
8.	Quercetin	302.040	7	5	2.155	0	Unviolated
9.	1-Methyl-2-pyrrolidineethanol	129.120	2	1	-0.220	0	Unviolated
10.	Favipiravir	157.030	5	3	-0.934	0	Unviolated
11.	2-Acetylpyrrolidine	113.080	2	1	-0.210	0	Unviolated
12.	2-Methoxy-4-vinylphenol	150.070	2	1	2.251	0	Unviolated
13.	Morpholine	87.070	2	1	-0.556	0	Unviolated

Results and Discussion

Lipinski’s Rule of Five

Among the tested bioactive compounds from *S. androgynus*, most showed no violations of Lipinski’s Rule of Five, indicating good potential for oral bioavailability. Two compounds, trifolin and astragalin, were found to violate the rule. Both possessed 11 HBA and 7 HBD, which might reduce membrane permeability and

lead to poor absorption, despite their known biological activity as natural flavonoid glycosides. In addition, afzelin also violated the HBD criterion with a value of 6. Drug-likeness plays an important role in the early stages of physicochemical property assessment in drug discovery. The HBA value indicates the number of oxygen and nitrogen atoms capable of accepting hydrogen bonds, whereas HBD reflects the number of hydroxyl (–OH) and amine (–NH)

groups capable of donating hydrogen atoms. In contrast, corchoionoside C, quercetin, kaempferol, favipiravir, 2,4-di-tert-butylphenol, 1-methyl-2-pyrrolidineethanol, 2-acetylpyrrolidine, 2-methoxy-4-vinylphenol, morpholine, and the native ligand fully comply with Lipinski's criteria,

suggesting balanced physicochemical characteristics and good potential for oral formulations. All compounds had a molecular weight below 500 Da, indicating their ability to permeate cell membranes efficiently and diffuse easily.

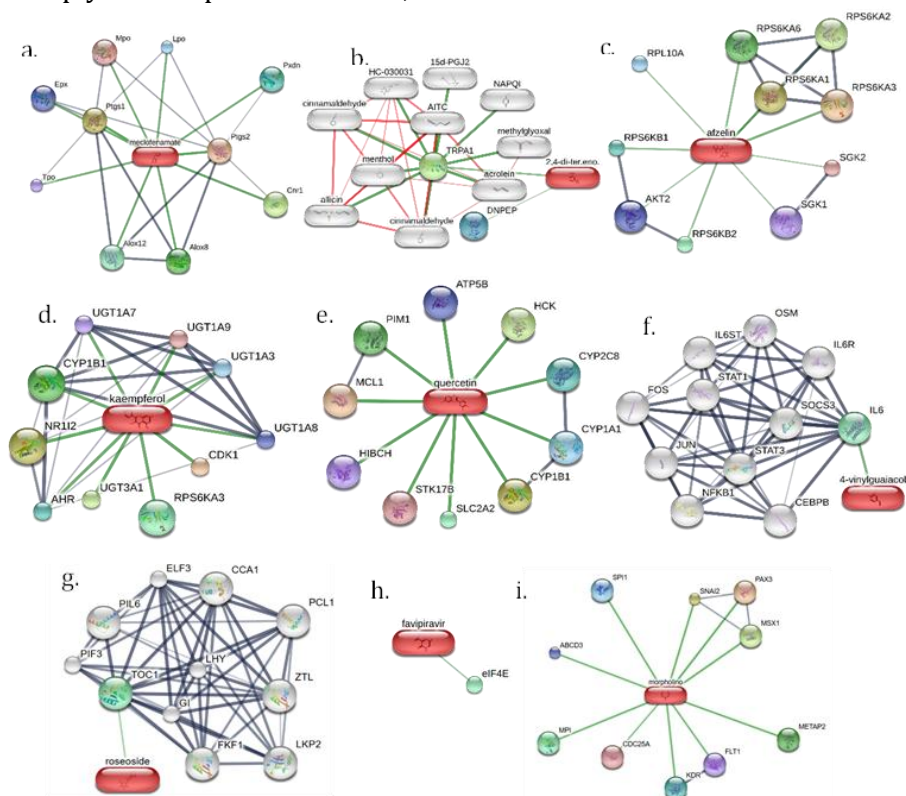


Figure 1. Protein–ligand interaction network using STITCH: (a) meclofenamic acid/meclofenamate, (b) 2,4-Di-tert-butylphenol, (c) afzelin, (d) kaempferol, (e) quercetin, (f) 2-Methoxy-4-vinylphenol/4-vinylguaiaicol, (g) corchoionoside C/roseoside, (h) favipiravir, and (i) morpholine.

Protein Network Analysis

STITCH integrates molecular, cellular, and phenotypic data related to small molecules and enables the exploration of interaction networks derived from known and predicted associations between chemicals and proteins (Kuhn et al., 2008). Figure 1a shows that meclofenamic acid has a strong affinity for key proteins involved in inflammatory regulation, particularly Ptgs1 and Ptgs2 (Dawidowicz et al., 2020). It also interacts with the Alox8 and Alox12 enzymes. Several *S. androgynus* compounds, such as 2,4-di-tert-butylphenol, afzelin, quercetin, kaempferol, and 2-methoxy-4-vinylphenol, were identified in the STITCH Homo sapiens database as potential anti-

inflammatory agents. Some compounds were also associated with protein kinases, including RPS6KA3 and RPS6KA1, which act as major downstream effectors in the Mitogen-Activated Protein Kinase (MAPK) signaling pathway. The interaction network further highlights the involvement of CYP1B1, CYP1A1, and IL-6, all of which play important roles in inflammatory regulation.

Favipiravir, corchoionoside C, and morpholine were not detected in Homo sapiens and appeared only in plant organisms. Meanwhile, 1-methyl-2-pyrrolidineethanol and 2-acetylpyrrolidine were not detected in STITCH at all. The absence of STITCH-mapped interactions does not necessarily indicate biological

irrelevance; rather, it may reflect limitations in available experimental annotations. These compounds may represent potential novel inhibitors that have not yet been experimentally validated or recorded in the STITCH database. Therefore, further confirmation through in vitro or in vivo studies is required.

Molecular Docking Calculation

The redocking process was carried out to validate and ensure the accuracy of the docking protocol used (Elalouf et al., 2024). Redocking was performed between the native ligand, meclofenamic acid, in the 5IKQ structure and the COX-2 receptor. The results are presented in Figure 2. Based on this figure, the conformations of meclofenamic acid before and after redocking show no significant differences. The RMSD obtained from the redocking process was 0.45 Å. The stability of the COX-2-meclofenamic acid complex is supported by two hydrogen-bond interactions involving the amino acid residues Ser530 and Tyr385. These findings are consistent with previous reports showing that Ser530 and Tyr385 are key residues involved in ligand interactions with the COX-2 receptor (Orlando & Malkowski, 2016). A valid redocking result must produce an RMSD value of less than 2 Å, indicating that the protocol used in this study is suitable for subsequent docking analysis.

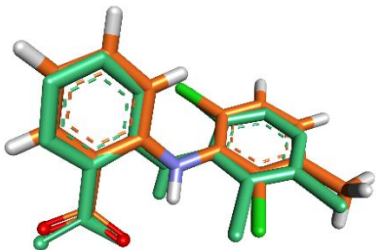


Figure 2. Superimposition of the native ligand (green) and the ligand after redocking (orange).

Molecular docking calculations were conducted to model the interaction between proteins and ligands (Nouredine et al., 2021). In this study, docking was performed between ten bioactive compounds from *S. androgynus* and the 5IKQ receptor. Table 2 summarizes the binding energy values of these compounds. All tested compounds exhibited negative binding energies, suggesting their potential as COX-2 enzyme inhibitors. Visualizations of the native ligand in 2D and 3D formats are provided in Figure 3. Among all compounds, corchoionoside C demonstrated the strongest affinity toward the target protein, with the lowest binding energy value of –9.57 kcal/mol. This value was lower than that of the native ligand, which showed a binding energy of –8.72 kcal/mol.

Table 2. Results of molecular docking calculations of bioactive compounds from *Sauropus androgynus* against the inflammatory COX-2 receptor.

No.	Compounds	PubChem ID	Binding Energy (kcal/mol)	Hydrogen Bonds
1.	Meclofenamic acid (native ligand)	4037	-8.72	Ser530; Tyr385
2.	2,4-Di-tert-butylphenol	7311	-7.29	Van der Waals: Arg513; Gln192; Ile517; Tyr355; Val349; Ala527
3.	Afzelin	5316673	-9.14	Ser353; Arg120; Phe518; Gln182
4.	Kaempferol	5280863	-8.2	Trp387;Ala199; Thr206; Asn382
5.	Corchoionoside C	10317980	-9.57	Tyr385; Trp387; Phe210
6.	Quercetin	5280343	-8.19	Met522; Val349; Phe518; Gln192
7.	1-Methyl-2- pyrrolidineethanol	93363	-4.89	Tyr385
8.	Favipiravir	492405	-4.81	Ser530; Asn375

9. 2-Acetylpyrrolidine	550747	-5.05	Trp387; Thr206
10. 2-Methoxy-4-vinylphenol	332	-5.64	Tyr385
11. Morpholine	8083	-4.52	Phe529; Asn375

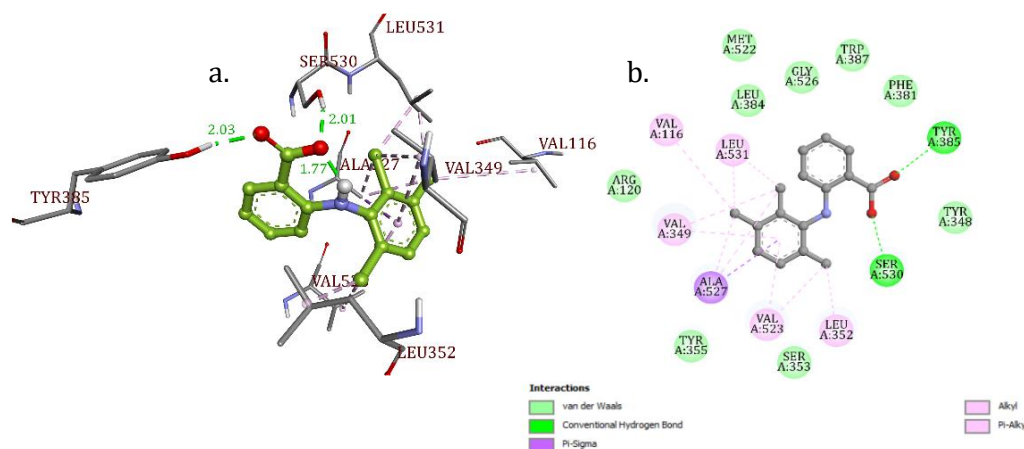


Figure 3. (a) Native ligand 3D complex, (b) Native ligand 2D complex

Lower binding energy indicates stronger ligand affinity, thereby increasing the likelihood of inhibition (Shivanika et al., 2022). The hydroxyl group ($-OH$) of corchoionoside C interacted at the active site through hydrogen bonds involving the amino acid residues Tyr385, Trp387, and Phe210, as visualized in Figure 4b. The bond lengths formed with these residues were 1.87, 1.67, and 2.00 Å, respectively, as shown in Figure 4a. The catalytic residue Tyr385 is associated with the conversion of arachidonic acid to prostaglandins through electron transfer to heme, initiating the formation of a tyrosyl radical at the COX active site (Harshitha et al., 2022).

Hydrogen bonds play a crucial role in drug-receptor interactions and in maintaining the structural stability of biological components such as proteins (Üst et al., 2024). The presence of these interactions may inhibit active sites and decrease COX enzymatic activity by reducing the synthesis of pro-inflammatory prostaglandins (Smith & Malkowski, 2019). Corchoionoside C is classified as a flavonoid. An experimental study by Gayathiri et al. (2024) demonstrated that bioactive compounds from *S. androgynus* exhibit anti-inflammatory activity and are capable of modulating pro-inflammatory mediators.

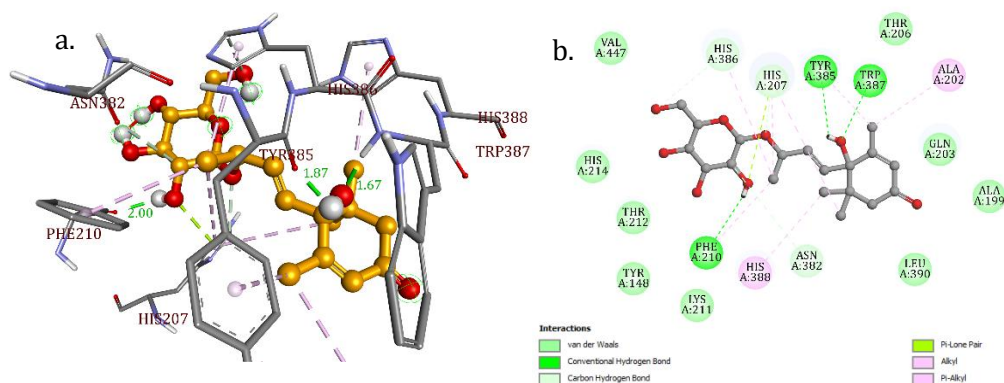


Figure 4. (a) Corchoionoside C 3D complex, (b) Corchoionoside C 2D complex.

The next compound identified with a relatively strong interaction toward the target receptor was afzelin, with a binding energy of -9.14 kcal/mol. Afzelin formed

four hydrogen bonds but did not share residue similarities with the native ligand in these interactions, as depicted in Figure 5. The amino acid residues involved and the

corresponding bond lengths were Ser353 (2.08 and 2.13 Å), Arg120 (3.00 and 2.76 Å), Phe518 (2.38 Å), and Gln182 (1.83 Å). Figure 5b illustrates the interaction types for each amino acid residue. A single amino acid residue may exhibit two different bond lengths due to intermolecular and intramolecular interactions. Khalipa et al. (2021) reported that afzelin provides a protective effect against UV-induced damage in human keratinocytes and epidermal equivalents, which is crucial in managing inflammation-related skin injuries. This compound also shows inhibitory activity against several pro-

inflammatory mediators such as tumor necrosis factor- α , IL-6, and PGE2.

Hong et al. (2025) further demonstrated through in vitro studies that afzelin modulates inflammatory and lipogenic responses, as indicated by reduced expression of IL-6, IL-1 β , and COX-2 in *Cutibacterium acnes* (SZ95)-stimulated sebocytes and particulate-treated cells. Afzelin also inhibits neuroinflammation by suppressing MAPK and NF- κ B phosphorylation signaling pathways (Lim et al., 2023). Meanwhile, quercetin, kaempferol, and 2,4-di-tert-butylphenol exhibit binding energies around -8 kcal/mol.

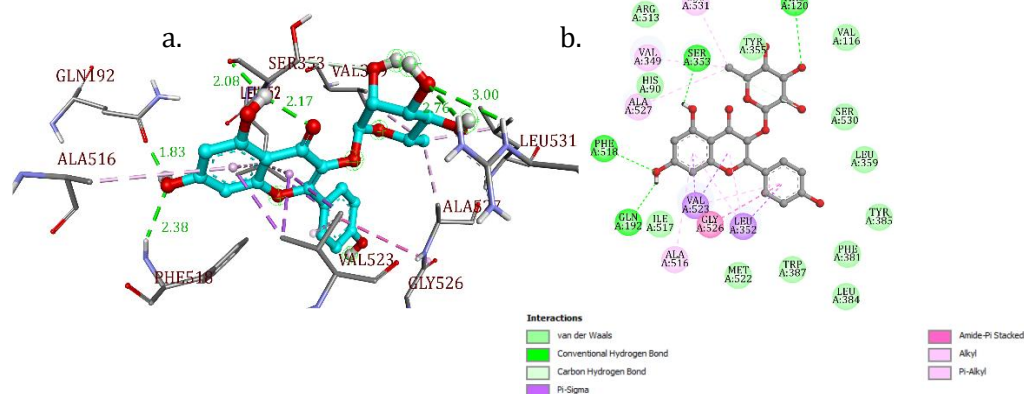


Figure 5. (a) Afzelin 3D complex, (b) Afzelin 2D complex.

Absorption, Distribution, Metabolism, Excretion, and Toxicity (ADMET)

The ADMET properties of a molecule describe its absorption, distribution, metabolism, excretion, and toxicity within the human body. These properties form the pharmacokinetic profile of a drug molecule and are essential for evaluating its pharmacodynamic activity. Based on Table 3, among all the medicinal chemistry parameters assessed, only corchoionoside C satisfied Lipinski's Rule of Five, Pfizer's rule, GSK's rule, and the Golden Triangle, indicating its potential suitability as an oral drug candidate. Afzelin violated the GSK rule due to its molecular weight of 432.110 Da. The GSK rule is fulfilled when $MW \leq 400$ and $\log P \leq 4$ (Abedin et al., 2024). Meanwhile, the native ligand violated two medicinal chemistry parameters, both the GSK and Pfizer rules. Afzelin also had a $\log P$ value of 5.133, which further violated the rule. The Pfizer and GSK rules predict that

meclofenamic acid may pose long-term side effects that should be carefully considered. Therefore, optimization of the formulation is required during drug development.

The human intestinal absorption (HIA) value indicates the extent to which an active compound is absorbed in the human intestine. A compound is classified as well absorbed when its HIA% falls within the acceptable range of -0.01 to 0. Poor absorption affects the compound's distribution and metabolism, which may increase the risk of neurotoxicity and nephrotoxicity (Utami et al., 2024). Corchoionoside C exhibited a poor HIA value because it exceeded the threshold, with a score of +0.903. All compounds showed low probability as P-glycoprotein (Pgp) inhibitors, while corchoionoside C and afzelin demonstrated high probability as Pgp substrates, with scores of 0.987 and 0.984, respectively.

Corchoionoside C showed a relatively low plasma protein binding (PPB) value of 68.847%. This PPB affinity reflects the compound's ability to bind strongly to plasma proteins (Veligeti et al., 2020). Meclofenamic acid, on the other hand, had a PPB value of more than 90%, indicating poor PPB characteristics. Highly bound compounds tend to remain in plasma and have limited penetration into peripheral tissues. Standard blood-brain barrier (BBB) permeability is considered good when the log BB value ranges from 0 to 0.3. As shown in Table 3, all compounds and the native ligand demonstrated acceptable BBB permeability, with log BB values of 0.154,

0.016, and 0.133, respectively. The volume of distribution (VD) parameter describes the compound's distribution capacity in vivo. A $VD < 0.07$ L/kg indicates strong plasma protein binding for highly hydrophilic compounds (Mashkani et al., 2023). Corchoionoside C and meclofenamic acid exhibited VD values of 0.515 and 0.268, respectively. Afzelin, however, showed a much higher VD value of 0.903, suggesting that the compound is lipophilic. The unbound fraction in plasma (F_u) is a key determinant of drug efficacy in pharmacokinetic and pharmacodynamic evaluations.

Table 3. ADMET prediction of *Sauropus androgynus* compounds.

Parameters	Corchoionoside C	Afzelin	Meclofenamic Acid
Medicinal Chemistry			
Lipinski rule	accepted	accepted	accepted
Pfizer rule	accepted	accepted	rejected
GSK rule	accepted	rejected	rejected
Golden triangle	accepted	accepted	accepted
Absorption			
Human intestinal absorption (HIA)	+++ (0.903)	-- (0.142)	--- (0.003)
Caco-2 permeability (log cm/s)	-5.714	-6.031	-4.472
P-glycoprotein inhibitor	-- (0.141)	--- (0.026)	--- (0.001)
P-glycoprotein substrate	+++ (0.984)	+++ (0.987)	--- (0.002)
F20%	--- (0.015)	--- (0.007)	--- (0.001)
F30%	+++ (0.969)	+++ (0.989)	--- (0.01)
Distribution			
Plasma protein binding (PPB) (%)	68.847	92.642	99.281
Blood-brain barrier penetration (BBB) (cm/s)	-- (0.154)	--- (0.016)	-- (0.133)
Volume distribution (L/kg)	0.515	0.903	0.268
F_u (%)	28.993	8.466	0.843

Metabolism			
CYP1A2 inhibitor	--- (0.008)	+ (0.556)	+ (0.502)
CYP1A2 substrate	-- (0.134)	--- (0.068)	++ (0.872)
CYP2C19 inhibitor	--- (0.02)	--- (0.043)	-- (0.191)
CYP2C19 substrate	++ (0.778)	--- (0.055)	-- (0.142)
CYP2C9 inhibitor	--- (0.003)	-- (0.229)	+ (0.699)
CYP2C9 substrate	--- (0.067)	++ (0.86)	++ (0.711)
CYP2D6 inhibitor	--- (0.001)	+ (0.528)	-- (0.245)
CYP2D6 substrate	--- (0.09)	--- (0.191)	-- (0.115)
CYP3A4 inhibitor	--- (0.008)	--- (0.311)	-- (0.109)
CYP3A4 substrate	-- (0.287)	--- (0.021)	-- (0.132)
Excretion			
Half-time (t1/2)	0.791	0.780	0.536
Clearance	1.790	5.030	1.217
Toxicity			
Human hepatotoxicity	-- (0.29)	-- (0.117)	++ (0.84)
hERG blockers	--- (0.034)	--- (0.034)	--- (0.06)
Rat oral acute toxicity	- (0.452)	-- (0.136)	++ (0.751)
AMES toxicity	-- (0.23)	++ (0.791)	--- (0.017)
Drug-induced liver injury	- (0.383)	+++ (0.978)	+++ (0.986)
Carcinogenicity	++ (0.885)	--- (0.059)	- (0.345)
FDAMDD	+++ (0.902)	--- (0.035)	-- (0.202)
Skin sensitization	-- (0.26)	++ (0.808)	+ (0.553)
Eye corrosion	--- (0.003)	--- (0.003)	--- (0.004)
Eye irritation	--- (0.015)	- (0.427)	--- (0.078)
Respiratory toxicity	+++ (0.913)	--- (0.059)	+++ (0.937)

Cytochrome P450 (CYP) is the most important enzyme family involved in drug metabolism, mediating the biotransformation of endogenous and xenobiotic compounds (Zhou et al., 2021). Approximately 75% of marketed drugs are metabolized by CYP enzymes, primarily through five major isoforms: CYP1A2, CYP3A4, CYP2C9, CYP2C19, and CYP2D6. Based on the prediction results, meclofenamic acid is identified as a substrate for CYP1A2 and an inhibitor of

CYP2C9. Meanwhile, corchoionoside C is predicted to function only as a substrate for CYP2C19, whereas afzelin acts as a substrate for CYP2C9. The excretion profile of a compound can be evaluated using total clearance and half-life parameters (Siswina et al., 2023). A shorter half-life indicates that the compound is less likely to accumulate excessively in the body, thereby reducing toxicity risks associated with accumulation. Corchoionoside C, afzelin, and meclofenamic acid exhibited half-lives of

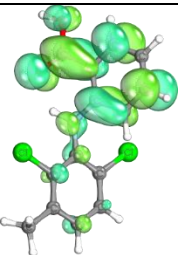
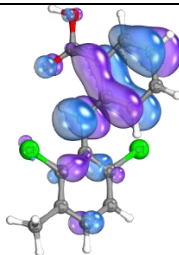
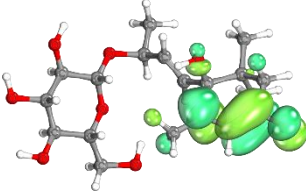
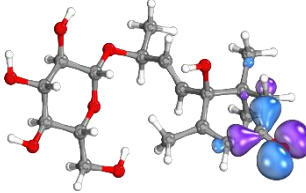
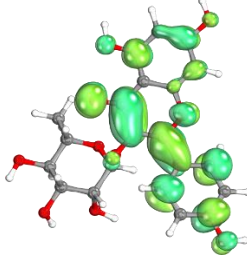
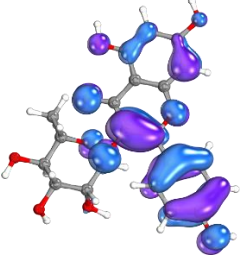
0.791, 0.780, and 0.536 hours, respectively. Afzelin demonstrated the highest total clearance at 5.030 mL/min/kg. A compound is considered favorable in this category if its clearance value is ≥ 5 mL/min/kg. In contrast, corchoionoside C and meclofenamic acid had clearance values

The potential compounds also show acceptable liver safety based on human hepatotoxicity predictions, although meclofenamic acid displays a positive (+) signal, suggesting a possible risk of liver damage. The drug-induced liver injury (DILI) score of 0.383 for corchoionoside C further indicates a low potential to cause hepatic injury. The Ames test prediction was used to evaluate the mutagenic potential of each compound for genotoxicity assessment.

Frontier Molecular Orbital (FMO)

FMO was computed based on the optimized structures. Electronic parameters were calculated using the DFT approach to describe the conductivity, biological properties, chemical reactivity, kinetic stability, and spectroscopic characteristics of the bioactive compounds. These parameters included the highest occupied molecular orbital (HOMO), lowest unoccupied molecular orbital (LUMO), and the energy gap (Isravel et al., 2021). FMO was calculated using Becke's three-parameter hybrid exchange–correlation functional (B3LYP)/6-31G based on the optimized geometry. The HOMO and LUMO energy levels were determined based on changes in orbital occupancy from filled to empty states (Shivaleela et al., 2023). The visualization of the HOMO, LUMO, and energy gap values is presented in Table 4.

Table 4. Frontier orbital interpretation of bioactive compounds in *Sauropus androgynus* based on DFT/B3LYP calculations.

Compounds	LUMO (eV)	HOMO (eV)	ΔE (eV)
Meclofenamic acid	 -1.358	 -5.612	4.254
Corchoionoside C	 -1.560	 -6.352	4.792
Afzelin	 -1.696	 -5.924	4.228

Meclofenamic acid, as the native ligand, had a HOMO value of -5.612 eV and a LUMO value of -1.358 eV. Corchoionoside C exhibited HOMO and LUMO values of -6.352 eV and -1.560 eV, respectively. Analysis of its orbital distribution shows that the HOMO is primarily centered on the carbonyl atom, whereas the LUMO is concentrated on the alkene group, indicating the presence of an electrophilic site in the LUMO region. In comparison, afzelin had a HOMO value of -5.924 eV and a LUMO value of -1.696 eV. The orbital distribution in afzelin is more delocalized throughout the molecular framework, rather than being localized on a specific functional group. This delocalization reflects strong electronic flexibility (Bakti & Martoprawiro, 2024).

The energy difference between the HOMO and LUMO orbitals, known as the energy gap, represents the molecular stability and plays a crucial role in

determining the spectroscopic behavior of a chemical structure (Ariefin & Alfanaar, 2023). Meclofenamic acid had a smaller energy gap (4.254 eV) than corchoionoside C (4.792 eV), indicating favorable molecular stability and electron transfer potential. Meanwhile, afzelin exhibited the smallest energy gap (4.228 eV), suggesting higher chemical reactivity and stronger intramolecular charge-transfer capabilities due to its conjugated system (Akbari et al., 2024). A smaller energy gap generally indicates that electron excitation occurs more readily and that intramolecular electronic transitions become more pronounced (Bakti & Martoprawiro, 2024). This is often associated with a higher excited-state dipole moment, which may enhance the compound's ability to interact with biological targets such as the COX-2 enzyme through polar or electrostatic interactions.

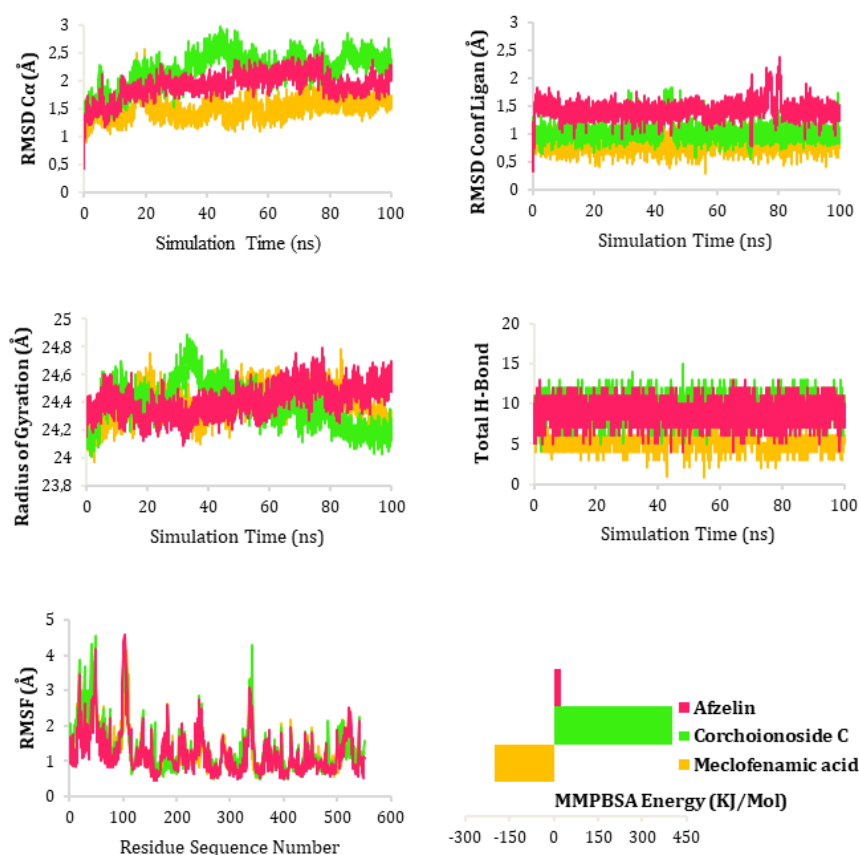


Figure 6. (a) Cα RMSD, (b) RMSD conf ligan, (c) Radius of gyration, (d) Total HBond, (e) RMSF, and (f) MMPBSA complex corchoionoside C and Afzelin to native ligand.

Molecular Dynamics Simulations

The movement of atoms is integrated through molecular dynamics simulations based on Newton's equations of motion (Puthanveedu & Muraleedharan, 2022). The thermodynamic stability trajectory over a 100 ns period was analyzed using parameters such as the number of hydrogen bonds, C α RMSD, ligand RMSD, radius of gyration, RMSF, and MMPBSA, as interpreted in Figure 5 (Sohrab & Kamal, 2022). Molecular dynamics simulations were performed on the conformers of corchoionoside C and afzelin, as both exhibited the lowest binding energies in the molecular docking calculations. Corchoionoside C formed the highest number of hydrogen bonds throughout most of the simulation, followed by afzelin, while the native ligand generated the lowest number of hydrogen bonds.

Stabilization of the protein structure through hydrogen bonding occurred between the hydrogen atoms of the amide group and the electronegative atoms of the carbonyl group in the protein backbone (Ghahremanian et al., 2022). At 48 ns, corchoionoside C successfully formed 15 hydrogen bonds. Hydrogen bonds contribute significantly to the stability and specificity of protein-ligand complexes and influence binding affinity as well as conformational changes. Corchoionoside C also showed a higher average number of hydrogen bonds (9.504) compared with afzelin (8.986). The average number of hydrogen bonds reflects the frequency and strength of possible interactions (Thapa et al., 2024). This suggests a stronger and broader interaction profile between corchoionoside C and the protein, potentially contributing to higher binding affinity and increased site stability. Hydrogen bonds play a central role in stabilizing protein-ligand complexes, particularly in terms of specificity, metabolic behavior, and bioavailability (Gayathiri et al., 2024). Therefore, hydrogen-bonding interactions are essential considerations in rational drug design.

The RMSD value during MD simulations is a critical parameter that

reflects the integrity of conformational stability. A low RMSD indicates a more stable complex, whereas wide oscillations or high RMSD values indicate instability in the protein-ligand complex (Azimi et al., 2021). Figure 6a shows that corchoionoside C exhibited the highest C α RMSD value at 2.96 Å. In contrast, meclofenamic acid and afzelin displayed lower maximum deviations of 2.56 Å and 2.47 Å, respectively.

In addition to calculating the RMSD of the entire complex, the YASARA program also allows ligand-specific RMSD analysis to evaluate conformational stability. Compounds from *S. androgynus* and the native ligand exhibited relatively stable ligand RMSD values. Figure 6b shows that afzelin experienced slight fluctuations during the 80 ns simulation period, although these changes were not significant. These conditions correlate with the binding energy data, which indicate that afzelin has a higher binding energy compared to corchoionoside C. This difference may be attributed to conformational adjustments in the afzelin ligand structure during the simulation. Meanwhile, corchoionoside C showed an RMSD range of 0.5–1.8 Å throughout the simulation.

The RMSF values indicate the mobility and flexibility of each amino acid residue in the protein throughout the simulation (Zrieq et al., 2021). The highest RMSF fluctuation was observed in the loop region at residue 33,825 of the corchoionoside C complex, with a value of 24.853 Å. High deviation and fluctuation during a simulation may indicate structural deformation and reduced stability. The RMSF counterplot of afzelin showed fluctuations of 4.56 and 4.29 Å at residues 48 and 341, respectively. The average root mean square distance between the center of gravity and the terminal atoms of the molecule represents the Radius of Gyration (Rg), which reflects the degree of compaction in the protein structure. The Rg profile indicates that all ligand-protein complexes exhibited stable values within the range of 24 to 24.9 Å.

MM-PBSA provides an integrated approach for calculating binding free energy, which is essential for evaluating the affinity between a ligand and its receptor (Rahman et al., 2021). The average MM-PBSA binding energies of the bioactive compounds in *S. androgynus* showed positive values, whereas meclofenamic acid, the native ligand, exhibited negative values. The MM-PBSA calculations in YASARA Dynamics employed the AMBER14 force field, where more positive binding energies indicate stronger ligand–target interactions. Corchoionoside C demonstrated an average MM-PBSA energy of 403.617 kJ/mol, while afzelin showed 25.441 kJ/mol. In contrast, the native ligand meclofenamic acid showed an average value of –198.629 kJ/mol.

Conclusion

The molecular docking results indicate that several compounds from *S. androgynus* exhibit lower binding energies than the native ligand. Corchoionoside C and afzelin emerged as the most potent COX-2 inhibitors, with binding energies of –9.57 and –9.14 kcal/mol, respectively. Protein network analysis using STITCH further confirmed interactions within the Homo sapiens biological system. Additional analysis revealed that the active site of corchoionoside C formed key hydrogen bond interactions with amino acid residues

Tyr385, Trp387, and Phe210, while afzelin interacted with Ser353, Arg120, Phe518, and Gln182, providing a molecular basis for their potential anti-inflammatory effects. These findings collectively highlight the promise of bioactive compounds from *S. androgynus*, particularly corchoionoside C and afzelin, as potential anti-inflammatory agents. Molecular dynamics simulations also demonstrate that the compound–protein complexes remained highly stable with minimal fluctuations throughout the simulation period, supporting their potential biological activity. The HOMO–LUMO analysis reflects the capacity of corchoionoside C and afzelin to interact with biological targets such as COX-2 through polar and electrostatic interactions, with afzelin exhibiting a lower energy gap than meclofenamic acid. Overall, these results support the biological potential of the identified compounds and justify further in vivo and in vitro experimental validation.

Acknowledgments

The authors express their gratitude to the Ministry of Religious Affairs The Awakened Indonesia Research Funds (MoRA The AIR Funds), and the Laboratory of the Faculty of Science and Technology, UIN Sultan Thaha Saifuddin Jambi, for providing the necessary facilities.

References

- Abedin, M. M., Pal, T. K., Chanmiya Sheikh, M., & Alam, M. A. (2024). Investigation on synthesized sulfonamide Schiff base with DFT approaches and in silico pharmacokinetic studies: Topological, NBO, and NLO analyses. *Heliyon*, 10(14), e34499. <https://doi.org/10.1016/j.heliyon.2024.e34499>
- Akbari, Z., Stagno, C., Iraci, N., Efferth, T., Omer, E. A., Piperno, A., Montazerzohori, M., Feizi-dehnayebi, M., & Micale, N. (2024). Biological evaluation, DFT, MEP, HOMO–LUMO analysis and ensemble docking studies of Zn (II) complexes of bidentate and tetradentate Schiff base ligands as antileukemia agents. *Journal of Molecular Structure*, 1301(December 2023), 137400. <https://doi.org/10.1016/j.molstruc.2023.137400>
- Ananda, A. N., Triawanti, T., Setiawan, B., Makati, A. C., Putri, J. A., & Raharjo, S. J. (2024). In silico study of the flavonoid compound of *Sauropus androgynus* leaves ON RNA-Dependent RNA polymerase (RdRp) SARS-CoV-2. *Aspects of Molecular Medicine*, 3(128), 100032. <https://doi.org/10.1016/j.amolm.2023.100032>
- Ariefin, M., & Alfanaar, R. (2023). Molecular Modelling Based on TD-DFT Applied to UV Spectra of Coumarin

- Derivatives. Walisongo Journal of Chemistry, 6(1), 61–68. <https://doi.org/10.21580/wjc.v6i1.15696>
- Awaludin, Kartina, Maulianawati, D., Manalu, W., Andriyanto, Septiana, R., Arfandi, A., & Lalang, Y. (2020). Phytochemical screening and toxicity of ethanol extract of *Sauropus androgynus*. Biodiversitas, 21(7), 2966–2970. <https://doi.org/10.13057/biodiv/d210712>
- Azimi, F., Ghasemi, J. B., Azizian, H., Najafi, M., Faramarzi, M. A., Saghaei, L., Sadeghi-aliabadi, H., Larijani, B., Hassanzadeh, F., & Mahdavi, M. (2021). Design and synthesis of novel pyrazole-phenyl semicarbazone derivatives as potential α -glucosidase inhibitor: Kinetics and molecular dynamics simulation study. International Journal of Biological Macromolecules, 166, 1082–1095. <https://doi.org/10.1016/j.ijbiomac.2020.10.263>
- Bakti, A. B., & Martoprawiro, M. A. (2024). Computational Study of The Effect of Structure on Antioxidant Activity and Drug Score of Coumarin Derivatives. Walisongo Journal of Chemistry, 7(2), 181–192. <https://doi.org/10.21580/wjc.v7i2.23327>
- Bommu, U. D., Konidala, K. K., Pamanji, R., & Yeguvapalli, S. (2017). Structural probing, screening and structure-based drug repositioning insights into the identification of potential Cox-2 inhibitors from selective coxibs. Interdisciplinary Sciences: Computational Life Sciences, 11(2), 153–169.
- Case, D. A., et al. (2016). AMBER 2016. San Fransisco.
- Chandwe, K., & Kelly, P. (2021). Colostrum therapy for human gastrointestinal health and disease. Nutrients, 13(6), 1–14. <https://doi.org/10.3390/nu13061956>
- Dassault Systemes. (2019). Biovia Discovery Studio Visualizer. San Diego.
- Dawidowicz, M., Kula, A., Świętochowski, P., & Ostrowska, Z. (2020). Assessment of the impact of PTGS1 , PTGS2 and CYP2C9 polymorphisms on pain , effectiveness and safety of NSAID therapies Ocena wpływu polimorfizmów PTGS1 , PTGS2 i CYP2C9 na ból , skuteczność i bezpieczeństwo terapii NLPZ. 504–516.
- Elalouf, A., Rosenfeld, A. Y., & Maoz, H. (2024). Targeting serotonin receptors with phytochemicals – an in-silico study. Scientific Reports, 14(1), 1–22. <https://doi.org/10.1038/s41598-024-76329-6>
- Fikri, F., & Purnama, M. T. E. (2020). Pharmacology and phytochemistry overview on sauropus androgynous. Systematic Reviews in Pharmacy, 11(6), 124–128. <https://doi.org/10.31838/srp.2020.6.20>
- Gayathiri, E., Prakash, P., Ahamed, M., Pandiaraj, S., Venkidasamy, B., Dayalan, H., Thangaraj, P., Selvam, K., Chaudhari, S. Y., Govindasamy, R., & Thiruvengadam, M. (2024). Multitargeted pharmacokinetics, molecular docking and network pharmacology-based identification of effective phytocompounds from *Sauropus androgynus* (L.) Merr for inflammation and cancer treatment. Journal of Biomolecular Structure and Dynamics, 42(15), 7883–7896. <https://doi.org/10.1080/07391102.2023.2243335>
- Ghahremanian, S., Rashidi, M. M., Raeisi, K., & Toghraie, D. (2022). Molecular dynamics simulation approach for discovering potential inhibitors against SARS-CoV-2: A structural review. Journal of Molecular Liquids, 354, 118901. <https://doi.org/10.1016/j.molliq.2022.118901>
- Harshitha, B. T., Jayashankar, J., Anand, A. P., Sandeep, S., Jayanth, H. S., Karthik, C. S., Mallu, P., Haraprasad, N., &

- Krishnamurthy, N. B. (2022). Structural and Functional Insights of Thiazole Derivatives as Potential Anti-inflammatory Candidate: A New Contender on Chronic and Acute SARS-CoV-2 Inflammation and Inhibition of SARS-CoV-2 Proteins. *Asian Journal of Chemistry*, 34(8), 1893–1920.
<https://doi.org/10.14233/ajchem.2022.23673>
- Hikmawanti, N, P, E., Hayati, & Andriyani, Y. (2021). Total Flavonoid Content in Hydro-ethanolic Extract of *Sauropus androgynus* (L.) Merr Leaves from Three Regions with Different Altitude. *Jurnal Jamu Indonesia*, 6(2), 61–67.
<https://doi.org/10.29244/jji.v6i2.195>
- Hong, J. Y., Choi, Y. H., Roh, Y. J., Lee, M. K., Zouboulis, C. C., & Park, K. Y. (2025). Effect of afzelin on inflammation and lipogenesis in particulate matter-stimulated C. acnes-treated SZ95 sebocytes. *Frontiers in Medicine*, 12.
<https://doi.org/10.3389/fmed.2025.1518382>
- Isravel, A. D., Jeyaraj, J. K., Thangasamy, S., & John, W. J. (2021). DFT, NBO, HOMO-LUMO, NCI, stability, Fukui function and hole – Electron analyses of tolcapone. *Computational and Theoretical Chemistry*, 1202(May), 113296.
<https://doi.org/10.1016/j.comptc.2021.113296>
- Jantarawong, S., Wathanaphanit, P., Panichayupakaranant, P., & Pengjam, Y. (2025). Prediction of ADMET profile and anti-inflammatory potential of chamuangone. *Scientific Reports*, 15(1), 1–15.
<https://doi.org/10.1038/s41598-025-86809-y>
- Ju, Z., Li, M., Xu, J., Howell, D. C., Li, Z., & Chen, F. E. (2022). Recent development on COX-2 inhibitors as promising anti-inflammatory agents: The past 10 years. *Acta Pharmaceutica Sinica B*, 12(6), 2790–2807.
<https://doi.org/10.1016/j.apsb.2022.01.002>
- Khalipa, A. B. R., Bhuia, M., Mondal, M., Hossain, M. S., Sakib, M. R., Prottay, A. S., Rahman, N., Rabbani, G., & Akter, K. (2021). in-Silico Molecular Docking Study of Afzelin and Its Derivatives Against 6M0J for Treatment of Covid-19. *International Journal of Evergreen Scientific Research Research Paper*, 03,62-77
- Knizia, G. (2013). Intrinsic atomic orbitals: An unbiased bridge between quantum theory and chemical concepts. *Journal of Chemical Theory and Computation*, 9(11), 4834–4843.
<https://doi.org/10.1021/ct400687b>
- Kuhn, M., Mering, C. Von, Campillos, M., & Jensen, L. J. (2008). STITCH : interaction networks of chemicals and proteins. 36(December 2007), 684–688.
<https://doi.org/10.1093/nar/gkm795>
- Land, Henrik, and M. S. H. (2017). YASARA: a tool to obtain structural guidance in biocatalytic investigations." *Protein engineering: methods and protocols*.
- Lee, S. Y., Cho, S. S., Li, Y. C., Bae, C. S., Park, K. M., & Park, D. H. (2020). Anti-inflammatory Effect of Curcuma longa and Allium hookeri Co-treatment via NF-κB and COX-2 Pathways. *Scientific Reports*, 10(1), 1–11.
<https://doi.org/10.1038/s41598-020-62749-7>
- Lim, H. J., Prajapati, R., Seong, S. H., Jung, H. A., & Choi, J. S. (2023). Antioxidant and Antineuroinflammatory Mechanisms of Kaempferol-3-O-β-d-Glucuronate on Lipopolysaccharide-Stimulated BV2 Microglial Cells through the Nrf2/HO-1 Signaling Cascade and MAPK/NF-κB Pathway. *ACS Omega*, 8(7), 6538–6549.
<https://doi.org/10.1021/acsomega.2c06916>
- Lipinski, C. A. (2004). Lead- and drug-like compounds: The rule-of-five revolution. *Drug Discovery Today: Technologies*, 1(4), 337–341.
<https://doi.org/10.1016/j.ddtec.2004.11.007>

- Mashkani, Z. S., Yali, Z. P., Dorgalaleh, A., & Shams, M. (2023). Evaluating the Potential Blood Coagulant Activity of *Caenothus americanus* Compounds: Computational Analysis using Docking, Physicochemical, and ADMET Studies. 1–47. <http://biorxiv.org/lookup/doi/10.1101/2023.09.05.555050>
- McEvoy, L., Carr, D. F., & Pirmohamed, M. (2021). Pharmacogenomics of NSAID-Induced Upper Gastrointestinal Toxicity. *Frontiers in Pharmacology*, 12(June), 1–15. <https://doi.org/10.3389/fphar.2021.684162>
- Mirza, F. J., Zahid, S., Amber, S., Sumera, S., Jabeen, H., Asim, N., & Ali Shah, S. A. (2022). Multitargeted Molecular Docking and Dynamic Simulation Studies of Bioactive Compounds from *Rosmarinus officinalis* against Alzheimer's Disease. *Molecules*, 27(21), 1–18. <https://doi.org/10.3390/molecules27217241>
- Morris, G. M., & Lim-Wilby, M. (2008). Molecular docking. In *Methods in Molecular Biology* (Vol. 443, pp. 365–382). https://doi.org/10.1007/978-1-59745-177-2_19
- Neese, F., Wennmohs, F., Becker, U., & Riplinger, C. (2020). The ORCA quantum chemistry program package. *Journal of Chemical Physics*, 152(22). <https://doi.org/10.1063/5.0004608>
- Noureddine, O., Issaoui, N., Gatfaoui, S., Al-Dossary, O., & Marouani, H. (2021). Quantum chemical calculations, spectroscopic properties and molecular docking studies of a novel piperazine derivative. *Journal of King Saud University - Science*, 33(2), 101283. <https://doi.org/10.1016/j.jksus.2020.101283>
- Orlando, B. J., & Malkowski, M. G. (2016). Substrate-selective inhibition of cyclooxygenase-2 by fenamic acid derivatives is dependent on peroxide tone. *Journal of Biological Chemistry*, 291(29), 15069–15081. <https://doi.org/10.1074/jbc.M116.725713>
- Pettersen, E. F., Goddard, T. D., Huang, C. C., Couch, G. S., Greenblatt, D. M., Meng, E. C., & Ferrin, T. E. (2004). UCSF Chimera - A visualization system for exploratory research and analysis. *Journal of Computational Chemistry*, 25(13), 1605–1612. <https://doi.org/10.1002/jcc.20084>
- Puthanveedu, V., & Muraleedharan, K. (2022). Phytochemicals as potential inhibitors for COVID-19 revealed by molecular docking, molecular dynamic simulation and DFT studies. *Structural Chemistry*, 33(5), 1423–1443. <https://doi.org/10.1007/s11224-022-01982-4>
- Rahman, M. M., Junaid, M., Zahid Hosen, S. M., Mostafa, M., Liu, L., & Benkendorff, K. (2021). Mollusc-derived brominated indoles for the selective inhibition of cyclooxygenase: A computational expedition. *Molecules*, 26(21). <https://doi.org/10.3390/molecules26216538>
- Shivaleela, B., Shivraj, G. G., & Hanagodimath, S. M. (2023). Estimation of dipole moments by Solvatochromic shift method, spectroscopic analysis of UV-Visible, HOMO-LUMO, ESP map, Mulliken atomic charges, NBO and NLO properties of benzofuran derivative. *Results in Chemistry*, 6(July), 101046. <https://doi.org/10.1016/j.rechem.2023.101046>
- Shivanika, C., Deepak Kumar, S., Ragunathan, V., Tiwari, P., Sumitha, A., & Brindha Devi, P. (2022). Molecular docking, validation, dynamics simulations, and pharmacokinetic prediction of natural compounds against the SARS-CoV-2 main-protease. *Journal of Biomolecular Structure and Dynamics*, 40(2), 585–611. <https://doi.org/10.1080/07391102.2020.1815584>

- Sinha, S. B., & Wang, T. and S. M. (2022). Applications of molecular dynamics simulation in nanomedicine. *Membranes*, 397–405. <https://doi.org/10.1016/B978-0-12-818627-5.00007-5>
- Siswina, T., Rustama, M. M., Sumiarsa, D., Apriyanti, E., Dohi, H., & Kurnia, D. (2023). Antifungal Constituents of *Piper crocatum* and Their Activities as Ergosterol Biosynthesis Inhibitors Discovered via In Silico Study Using ADMET and Drug-Likeness Analysis. *Molecules*, 28(23). <https://doi.org/10.3390/molecules28237705>
- Smith, W. L., & Malkowski, M. G. (2019). Interactions of fatty acids, nonsteroidal anti-inflammatory drugs, and coxibs with the catalytic and allosteric subunits of cyclooxygenases-1 and -2. *Journal of Biological Chemistry*, 294(5), 1697–1705. <https://doi.org/10.1074/jbc.TM118.006295>
- Sohrab, S. S., & Kamal, M. A. (2022). Screening, Docking, and Molecular Dynamics Study of Natural Compounds as an Anti-HER2 for the Management of Breast Cancer. *Life*, 12(11). <https://doi.org/10.3390/life12111729>
- Tai, F. W. D., & McAlindon, M. E. (2021). Non-steroidal anti-inflammatory drugs and the gastrointestinal tract. *Clinical Medicine, Journal of the Royal College of Physicians of London*, 21(2), 131–134. <https://doi.org/10.7861/CLINMED.2021-0039>
- Thapa, S., Biradar, M. S., Nargund, S. L., Ahmad, I., Agrawal, M., Patel, H., & Lamsal, A. (2024). Synthesis, Molecular Docking, Molecular Dynamic Simulation Studies, and Antitubercular Activity Evaluation of Substituted Benzimidazole Derivatives. *Advances in Pharmacological and Pharmaceutical Sciences*, 2024. <https://doi.org/10.1155/2024/9986613>
- Trabalzini, L. (2020). Progression and Immunity. 1–26.
- Ur Rashid H, Xu Y, Ahmad N, Muhammad Y, Wang L (2019) Promising anti-inflammatory effects of chalcones via inhibition of cyclooxygenase, prostaglandin E2, inducible NO synthase and nuclear factor kb activities. *Bioorg Chem* 87:335–365. <https://doi.org/10.1016/j.bioorg.2019.03.033>
- Üst, Ö., Yalçın, E., Çavuşoğlu, K., & Özkan, B. (2024). LC-MS/MS, GC-MS and molecular docking analysis for phytochemical fingerprint and bioactivity of *Beta vulgaris* L. *Scientific Reports*, 14(1), 1–17. <https://doi.org/10.1038/s41598-024-58338-7>
- Utami, W., Apriyanto, Antari, L., Rasyid, H., & Fitriani, I. N. (2024). Inhibition of Human Acetylcholinesterase (4EY7) using Bioactive Compound from *Moringa oleifera*: Molecular Docking and Dynamic Studies. *Jurnal Kimia Valensi*, 10(2), 290–303. <https://doi.org/10.15408/jkv.v10i2.39840>
- Utami, W., Aziz, H. A., Fitriani, I. N., Zikri, A. T., Mayasri, A., & Nasrudin, D. (2020). In silico anti-inflammatory activity evaluation of some bioactive compound from *ficus religiosa* through molecular docking approach. *Journal of Physics: Conference Series*, 1563(1). <https://doi.org/10.1088/1742-6596/1563/1/012024>
- Veligeti, R., Madhu, R. B., Anireddy, J., Pasupuleti, V. R., Avula, V. K. R., Ethiraj, K. S., Uppalanchi, S., Kasturi, S., Perumal, Y., Anantaraju, H. S., Polkam, N., Guda, M. R., Vallela, S., & Zyryanov, G. V. (2020). Synthesis of novel cytotoxic tetracyclic acridone derivatives and study of their molecular docking, ADMET, QSAR, bioactivity and protein binding properties. *Scientific Reports*, 10(1), 1–22.

- <https://doi.org/10.1038/s41598-020-77590-1>
- Xia, F., Li, B., Song, K., Wang, Y., Hou, Z., Li, H., Zhang, X., Li, F., & Yang, L. (2024). Polyploid Genome Assembly Provides Insights into Morphological Development and Ascorbic Acid Accumulation of *Sauropus androgynus*. *International Journal of Molecular Sciences*, 25(1), 1–18. <https://doi.org/10.3390/ijms25010300>
- Yucel, Turan, N., Al, A., Asfour, R., Evrim, A., Kandemir, Ü., Ozkay, Ü. D., Can, D., & Yurttas, L. (2024). Bioorganic Chemistry Design and synthesis of novel dithiazole carboxylic acid Derivatives: In vivo and in silico investigation of their Anti-Inflammatory and analgesic effects. 144(December 2023). <https://doi.org/10.1016/j.bioorg.2024.107120>
- Zhang, J., Zhu, W., Zhu, W., Yang, P. P., Xu, J., Manosroi, J., Kikuchi, T., Abe, M., Akihisa, T., Feng, F., Chemistry, N. M., Materials, B. F., Mai, C., Sciences, P., & Merr, L. (n.d.). Article Type: Full Paper Melanogenesis-inhibitory and cytotoxic activities of chemical constituents from the leaves of. <https://doi.org/10.1111/ijlh.12426>
- Zhou, Y., Khan, H., Xiao, J., & Cheang, W. S. (2021). Effects of arachidonic acid metabolites on cardiovascular health and disease. *International Journal of Molecular Sciences*, 22(21). <https://doi.org/10.3390/ijms222112029>
- Zrieq, R., Ahmad, I., Snoussi, M., Noumi, E., Iriti, M., Algahtani, F. D., Patel, H., Saeed, M., Tasleem, M., Sulaiman, S., Aouadi, K., & Kadri, A. (2021). Tomatidine and patchouli alcohol as inhibitors of SARS-CoV-2 enzymes (3CLpro, PLpro and NSP15) by molecular docking and molecular dynamics simulations. *International Journal of Molecular Sciences*, 22(19). <https://doi.org/10.3390/ijms221910693>